



# Design optimization of ink in electrohydrodynamic jet printing: Effect of viscoelasticity on the formation of Taylor cone jet



Milim Yu, Kyung Hyun Ahn<sup>\*</sup>, Seung Jong Lee

School of Chemical and Biological Engineering, Institute of Chemical Process, Seoul National University, Seoul 151-744, Republic of Korea

## ARTICLE INFO

### Article history:

Received 7 March 2015

Received in revised form 25 September 2015

Accepted 26 September 2015

Available online 30 September 2015

### Keywords:

Ink viscoelasticity

Taylor cone jet

Operating window map

Electrohydrodynamic printing

## ABSTRACT

The formation of Taylor cone jet is a key process in electrohydrodynamic printing that is used to produce high resolution patterns. Even though the inks are complex fluids composed of particles, binder, and solvent, most of previous researches have assumed the ink as a Newtonian fluid. In this study, we investigate the effect of viscoelasticity of the ink on Taylor cone jet using two model systems designed to control the elasticity and viscosity of the ink independently. The elasticity and viscosity improve the stability by expanding the operating windows for Taylor cone jet. The results can be summarized in terms of two parameters: elasticity parameter,  $\xi$ , and viscosity parameter,  $\chi$ . The increase in elasticity widens the range of voltage for Taylor cone jet zone, while the range of flow rate remains independent of elasticity. The effect of elasticity is dominant for  $\xi > 1$  while it is nearly negligible for  $\xi < 1$ . When the viscosity is increased, the Taylor cone jet zone is widened mainly by the flow rate when  $\chi < 1$ , while the voltage stabilizes the Taylor cone jet for  $\chi > 1$ . This study will contribute to the optimal design of EHD printing ink by providing the operating window maps in terms of material properties.

© 2015 Elsevier Ltd. All rights reserved.

## 1. Introduction

Electrohydrodynamic (EHD) printing has received an enormous attention due to its potential to provide high resolution patterns with a size ranging from as high as hundreds of micrometers down to tens of nanometers [1–3]. Industry insiders have considered it as an alternative process to inkjet printing because it can overcome the inherent limitation of the conventional inkjet printing associated with the size of a nozzle, which determines high resolution patterning [4–6].

The core principle of EHD printing is the formation of the cone jet which is generated by an electric potential between the nozzle and the substrate. The electric stress caused by the electric potential can change the shape of the ink from droplet to conical shape known as “Taylor cone” [7–10]. The electrified jet, which has much smaller diameter than the nozzle diameter, can be produced and printed by forming Taylor cone jet, while the droplet diameter from the ink jet printing swells 2 to 3 times larger than the nozzle diameter.

Finding the proper operating conditions is of a great importance in obtaining a stable Taylor cone jet. It is very challenging because the formation of Taylor cone jet and the printing quality are affected by many factors as follows: operating factors (flow rate, voltage) [11–15]; geometry factors (nozzle diameter, distance between nozzle and substrate)

[6,16]; and the physical properties of the ink (viscoelasticity [17–19], viscosity [20,21], conductivity [22–24], surface tension [25], dielectric property [26,27], density). The physical properties of the ink, in specific, influence the stability of Taylor cone jet, which is an outcome of multi-disciplinary subjects of electrostatics, electrokinetics, and fluid dynamics [28].

As the ink includes functional particles and polymers, it can be classified as a complex fluid [29,30]. The viscoelasticity of the ink can induce many unexpected phenomena in printing process, thus it should be included as a key material property together with all the associated factors that affect EHD printing process. However, most researches on EHD printing have assumed the ink as a simple Newtonian fluid [31, 32]. A few considered viscoelastic inks, but the effect of elasticity and viscosity has never been probed separately.

In this study, we explored the effect of viscoelasticity on the formation of Taylor cone jet using the well characterized model systems of low viscosity elastic polymer solutions. Two model systems were designed such that elasticity and viscosity varied independently, while all the other material properties were kept constant. All the variables associated in EHD printing process were restructured systematically in terms of seven dimensionless numbers. We first overviewed the new aspects of cone jet evolution rising from adopting the viscoelastic fluid assumption. We plotted the operating window maps for all sets of model fluids. As the elasticity and viscosity of the ink changed in each system, the optimum operating condition for the Taylor cone jet formation was determined quantitatively in terms of dimensionless numbers.

<sup>\*</sup> Corresponding author.

E-mail address: [ahnnet@snu.ac.kr](mailto:ahnnet@snu.ac.kr) (K.H. Ahn).

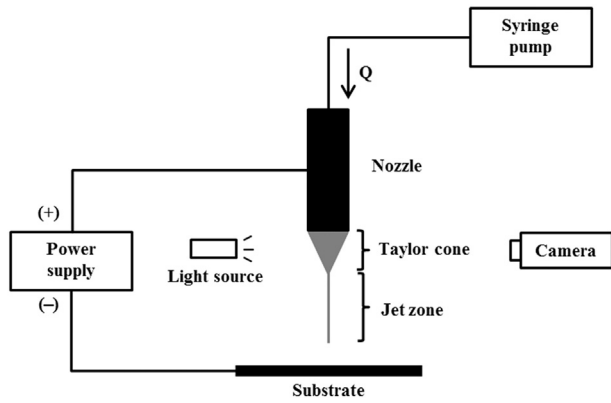


Fig. 1. Schematics for the EHD printing experimental setup.

## 2. Experimental

### 2.1. Materials and characterization

The low viscosity elastic fluids tested in this study were dilute solutions of polyethylene oxide (PEO) (supplied by Aldrich Chemical) with molecular weight ranging from  $3.0 \times 10^5$  to  $5.0 \times 10^6$  g/mol in 50 wt.% water/50 wt.% glycerol mixture. Polymer solutions were prepared at various concentrations of PEO and NaCl to obtain a wide range of solution properties. Polymer solutions were stirred for 72 h using a magnetic stirrer. The shear viscosities of PEO solutions were measured using a strain-controlled rotational rheometer (ARES, TA instruments, USA) with a conical fixture of 50 mm diameter and 0.04 rad cone angle. The viscosity of PEO solution with molecular weight  $5.0 \times 10^6$  g/mol showed slight shear thinning. Other polymer solutions showed constant viscosity in the shear rate range from 1 to  $100 \text{ s}^{-1}$ . Dielectric analyzer (SI 1260, Solartron, U.K.) was used to measure conductivity and permittivity. Surface tension was measured using a surface tensionmat (Fisher Scientific, U.K.).

### 2.2. Apparatus

The schematic diagram of the experimental setup is shown in Fig. 1. The liquid is supplied to the stainless steel capillary nozzle (inner diameter of 180  $\mu\text{m}$  and outer diameter of 300  $\mu\text{m}$ ) at a constant volumetric flow rate using a digitally controlled syringe pump (Longer Pump, Model LSP02-1B). A high voltage is applied between a conducting nozzle and a copper plate. The working distance between the nozzle and the substrate is 25 mm. The jetting mode is observed and simultaneously photographed using a high-speed camera (Photron® fastcam-ultima 512) with  $512 \times 512$  resolution and micro-zoom lens ( $6.5\times$ ). Light source (MORITEX, 250W Metal Halide lamp) is set up on the opposite side of the camera.

**Table 1**  
Model system I. Characteristic properties of PEO solutions with various molecular weight: molecular weight ( $M_w$ ), polymer weight concentration ( $c$ ), dimensionless concentration ( $c/c^*$ ), intrinsic viscosity ( $[\eta]$ ), solvent viscosity ( $\eta_s$ ), zero shear viscosity ( $\eta_0$ ), Zimm relaxation time ( $\lambda$ ), electric conductivity ( $\kappa$ ), surface tension ( $\gamma$ ) and relative permittivity ( $\epsilon'$ ).

| Code name | $M_w$<br>(g/mol)  | $c$<br>(wt.%) | $c/c^*$ | $[\eta]$<br>(ml/g) | $\eta_s$<br>(cp) | $\eta_0$<br>(cp) | $\lambda = t_\lambda$<br>(s) | $\kappa$<br>( $\mu\text{S/cm}$ ) | $\gamma$<br>(mN/m) | $\epsilon'$    |
|-----------|-------------------|---------------|---------|--------------------|------------------|------------------|------------------------------|----------------------------------|--------------------|----------------|
| M03       | $3.0 \times 10^5$ | 0.82          | 2.13    | $2.6 \times 10^2$  | $5.0 \pm 1.8$    | $22.0 \pm 2.3$   | $5.1 \times 10^{-5}$         | $24.0 \pm 1.8$                   | $56.0 \pm 2.5$     | $79.1 \pm 2.7$ |
| M06       | $6.0 \times 10^5$ | 0.57          | 2.33    | $4.1 \times 10^2$  |                  |                  | $1.6 \times 10^{-4}$         |                                  |                    |                |
| M10       | $1.0 \times 10^6$ | 0.38          | 2.16    | $5.7 \times 10^2$  |                  |                  | $3.7 \times 10^{-4}$         |                                  |                    |                |
| M20       | $2.0 \times 10^6$ | 0.26          | 2.34    | $9.0 \times 10^2$  |                  |                  | $1.2 \times 10^{-3}$         |                                  |                    |                |
| M40       | $4.0 \times 10^6$ | 0.17          | 2.42    | $1.4 \times 10^3$  |                  |                  | $4.2 \times 10^{-3}$         |                                  |                    |                |
| M50       | $5.0 \times 10^6$ | 0.15          | 2.41    | $1.6 \times 10^3$  |                  |                  | $5.3 \times 10^{-3}$         |                                  |                    |                |

Critical overlap concentration ( $c^*$ ) was calculated by classification of Flory for flexible polymer solutions, which is defined as  $c^* = 1/[\eta]$  [37,38]. It is widely accepted for dilute and semi-dilute polymer solutions.  $[\eta]$  is the intrinsic viscosity of polymer solution which depends on the molar mass of the chain according to the Mark-Houwink-Sakurada equation, where  $[\eta] = 0.072M_w^{0.65}$  for PEO solution in water/glycerol mixture [37].

### 2.3. Model systems

Two model systems were designed to analyze a) the effect of elasticity (model system I) and b) the effect of viscosity (model system II) independently. The concentration of ink was adjusted within the semi-dilute regime where the stable jet can be generated without spinning or bead jet [33–36]. In the first model system, the elasticity of the ink was controlled by changing polymer relaxation time which practically reflects the elasticity. The relaxation time in the semi-dilute region was estimated by the Zimm relaxation time, which can be calculated from the molecular weight and solvent viscosity [37]. Because of constant solvent viscosity in this system, the Zimm relaxation time depends only on the molecular weight of the polymer. Six PEO solutions with different molecular weight were prepared and their viscosity were adjusted to be constant by fixing the reduced concentration,  $c/c^* \sim 2.2 \pm 0.2$ , where  $c^*$  is the critical overlap concentration (explained in Table 1). The material properties of the model inks are listed in Table 1. Here, for example, M10 means the PEO solution of molecular weight  $1.0 \times 10^6$  g/mol. The text in parenthesis refers to unit.

In the second model system, the viscosity of the ink was controlled by changing polymer concentration. Six PEO solutions of different concentration were prepared and their elasticity were adjusted to be constant by fixing the molecular weight of PEO ( $M_w = 1.0 \times 10^6$  g/mol). The material properties of the model inks are listed in Table 2. Here, for example, C18 indicates the PEO solution of 0.18 wt.%. In both systems, other physical properties of the inks were controlled to be almost the same. The conductivity was fixed by controlling the amount of salt addition. Dielectric constant and surface tension and were constant because they are determined by the solvent. The addition of a small amount PEO had no effect on the surface tension and the dielectric constant.

### 3. Dimensional analysis

Dimensionless numbers were organized to systemize all the variables that affect the EHD printing. Using the Buckingham  $\pi$  theorem, the number of dimensionless groups could be determined as the number of variables minus the number of fundamental dimensions. The variables are:

$$Q, V, \lambda, \eta, \kappa, \gamma, \rho, \epsilon', \epsilon_0, d, L \quad (1)$$

where  $Q$  is the flow rate,  $V$  is the voltage,  $\lambda$  is the Zimm relaxation time,  $\eta$  is the viscosity,  $\kappa$  is the conductivity,  $\gamma$  is the surface tension,  $\rho$  is the density,  $\epsilon'$  is the permittivity of fluid,  $\epsilon_0$  is the permittivity of the surrounding air,  $d$  is the diameter of the nozzle, and  $L$  is the separation distance of the nozzle and the counter-electrode. As eleven variables contain four fundamental dimensions,  $[M]$ ,  $[L]$ ,  $[T]$ , and  $[V]$ , seven dimensionless numbers could be derived and the results are summarized in Table 3.

Dimensionless flow rate ( $\alpha$ ) and dimensionless voltage ( $\beta$ ) are the main process parameters.  $\alpha$  is defined as the ratio of supplied flow

Download English Version:

<https://daneshyari.com/en/article/7219639>

Download Persian Version:

<https://daneshyari.com/article/7219639>

[Daneshyari.com](https://daneshyari.com)